Cover Letter

We hereby declare that there is no duplicate publication elsewhere of any part of this work. There are no commercial relationships which might lead to a conflict of interests. The typescript has been read and agreed by all authors.

Authors' contributions:

Huawei Wang: Designed the study and developed the technical details; analyzed the motion data and performed the identifications; drafted the manuscript.

Antonie J. van den Bogert: Convinced the original idea and supervised the study; Revised the manuscript; approved the final version for submission.

Authors:

Huawei Wang

Antonie J. van den Bogert

Corresponding author:

Huawei Wang

Huawei.wang.buaa@gmail.com

Washkewicz College of Engineering

Cleveland State University

WH121, 2300 Chester Avenue, Cleveland OH, U.S. 44115-2214.

Referee Suggestions

Jerry Pratt: jpratt@ihmc.us (leader of ihmc humanoid robot project)

Twan Koolen: tkoolen@mit.edu (first author of the 2012 capture theory paper)

Art Kuo: arthur.kuo@ucalgary.ca

Manoj Srinivasan: srinivasan.88@osu.edu

Chenglong Fu: fcl@mail.tsinghua.edu.cn (my previous research advisor in China)

Manuscript

Identification of A Foot Placement Controller in Human Walking

Huawei Wang and Antonie J. van den Bogert

Mechanical Engineering, Washkewicz College of Engineering Cleveland State University, U.S.

Submitting for Original Article

Word count: around 3900 (needs to reduce to 3500)

CORRESPONDING AUTHOR:

Huawei Wang

Washkewicz College of Engineering

Cleveland State University

WH121, 2300 Chester Avenue, Cleveland OH, U.S. 44115-2214.

huawei.wang.buaa@gmail.com

Phone +1 216-262-8178

ABSTRACT

Step strategy is essential for both human beings and humanoid robots to keep walking balance. Although the capture theory has been developed as a successful step strategy for humanoid robots to keep walking balance under unpredictable environment, we are curious whether human beings use the same control algorithm to choose their foot placements. In this study, step controllers that have the same control structure as the capture theory were identified on 27 trials of perturbed walking data (nine participants, three speeds) through the closed-loop identification approach. The identified step controllers were able to drive a seven-link nonlinear gait model generating almost identical perturbation responses as the testing participants. In addition, identified step control gains are similar among participants and have relatively close but smaller values comparing to the capture theory, which means that the capture point is not a bad estimation but a little bit conservative in explaining humans' choice. Identification results also showed that the step control gains vary based on walking speed, which suggests that human choosing their foot placement does not based on a linear function of the feedback signals, but rather a nonlinear function. Lastly, identified control gains are consistent among multiple periods of perturbed walking data.

Keywords:

Step Strategy; Walking Balance; Capture Theory; Indirect Identification; Perturbed Walking Data;

1. INTRODUCTION

Fall has been a main issue for humanoid robots ever since they were first created. Step strategy is one of several strategies that can help solve the issue (Townsend 1985, Kuffner 2002, Sugihara 2002, Stephens 2007). Concept of the step strategy is simple, which is to control the swing leg to take a step. In general, fall of humanoid robots and humans can always be prevented if the swing leg can step to the right location at the right timing. However, finding a useful control algorithm for the step strategy that can achieve stable walking could be difficult, especially in the case of unpredictable environment. One of the most successful attempts is the capture theory (Pratt 2006), in which it predicts the desired foot placement based on a linear inverted pendulum (LIP) model (Kajita 2001). Both simulation and hardware tests have proved its usefulness in humanoid robots to maintain stable walking under external perturbations (Pratt 2012). Nonetheless, the algorithm for estimating the desired foot placement inside the capture theory includes many assumptions. For instance, estimation of the desired foot placement is based on the capture point, in which the LIP will stop (captured) at the middle stance (Pratt 2006, Koolen 2012). While, healthy humans' center of mass (CoM) tends to keep a relatively constant speed during the entire gait period. In addition, the swing leg dynamics and the landing energy lost (heel strike) were not considered (Zhang 2018, Kuo 2005). Studies have pointed out that humans do not step on the capture point or the extrapolated center of mass (XCoM), but behind and outward of them (Hof 2005, Hof 2008).

To understand what step strategy does humans use to keep walking balance, phase depended step controllers were extracted from both unperturbed and randomly perturbed walking data through linear models (Wang 2014, Joshi 2019, Seethapathi 2019). They

showed that linear feedbacks from the changes of pelvis position and velocity have encouraging correlations with the changes of foot placement. Their work also revealed that the step strategy of humans can be directly extract from walking data. However, these phases depended step controllers may not be able to explain the correct foot placement when walking at a randomly perturbed situation. That is say the perturbation continuously exists among all gait phases. Furthermore, linear model may not be sufficient as the plant model to represent how human choose their foot placements which have resulted poor fit (Joshi 2019). Therefore, identifying the phase-independent step controllers is essential to understand how human beings choose their foot placements under a randomly perturbed environment and to provide useful control algorithms for humanoid robots.

The purpose of this paper is to quantitively extract the phase-independent step strategy controllers from human walking data. To achieve this, we identified step strategy controllers from randomly perturbed walking data with a nonlinear gait model through the indirect identification approach. The identified step controllers have the same feedback structure as the capture theory, but their feedback gains were identified from the perturbed walking data. The indirect identification approach guarantees that the identified step controllers are able to drive the nonlinear gait model generating expecting motion (van der Kooij 2008). Identification results showed that human beings use relatively close but smaller feedback gains to find the foot placement comparing to the capture theory. Center of mass (CoM) position and velocity are sufficient as feedback signals to have a good foot placement estimation. However, the feedback control is more likely to be a nonlinear function, rather than the linear function suggested by the capture theory.

2. METHOD

Diagram plot of the indirect approach for the step controller identification is shown in Figure 1. The step strategy control gains were identified through trajectory optimization process. We assume that the correct step controllers are found if the nonlinear gait model can reproduce the motion of testing participants under the same perturbation. Therefore, the goal of this paper is to optimize the control parameters inside the locomotion controller to minimize the difference between the joint motion of the simulation model and the experimental data.

Figure 1 – Plot diagram of the indirect identification approach in walking step strategy identification. There are two components in the identification: One is the simulation model which includes the human body dynamics and the locomotion control (the step strategy algorithm). Another component is the experimental data which includes participants' reaction during perturbed walking experiment. The overall goal of the indirect approach is to minimize the difference between the outputs of the simulation model and experimental data by optimizing the control parameters .

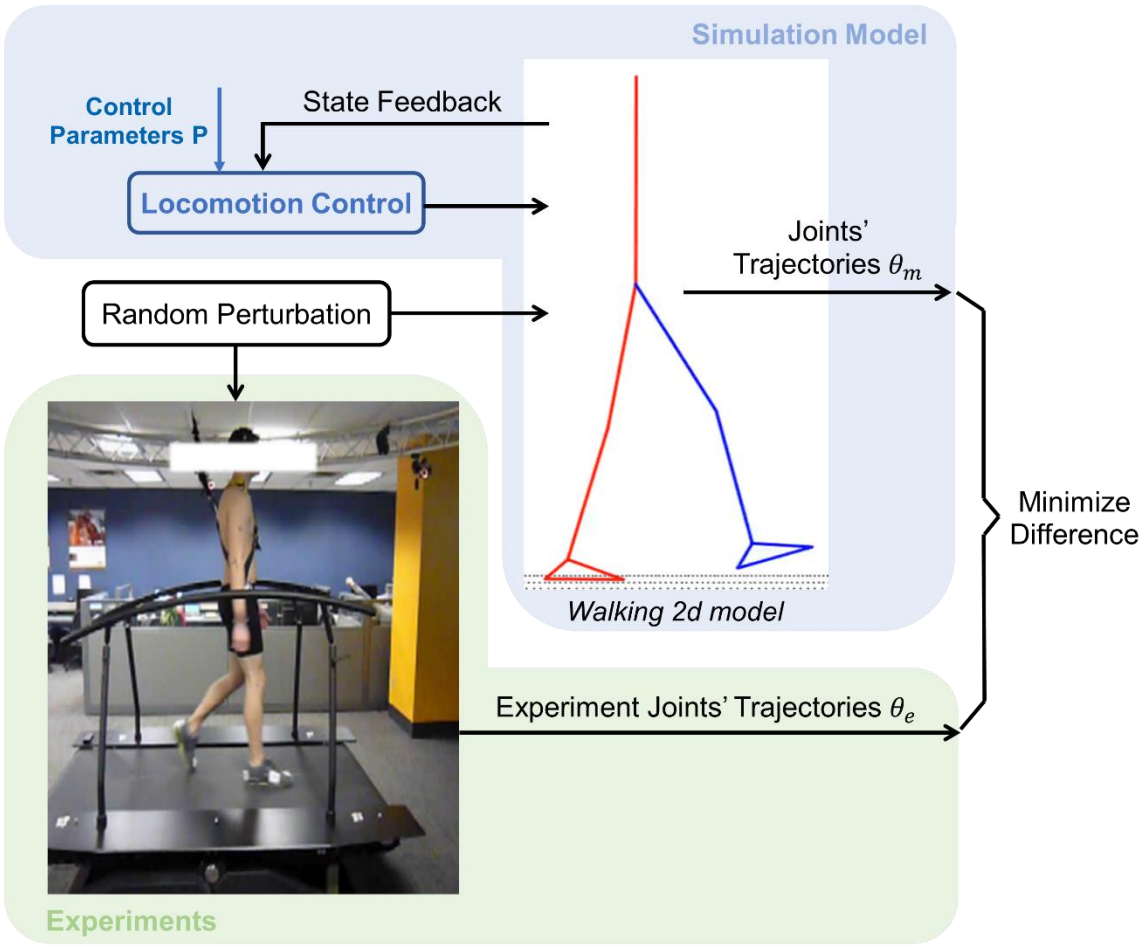

2.1. Experimental Data

Data used in this study is from a randomly perturbed walking experiment conducted by Moore et al. (Moore 2015). In the experiment, participants' reactions were recorded while they were walking on a treadmill with continuously perturbed walking speed. Each participant was tested under three baseline speeds: 0.8m/s, 1.2m/s, and 1.6m/s. The motion capture system (Motion Analysis) and 47 markers were used to track participants' full-body motion. An instrumented treadmill (Motekforce) was used performing the speed perturbation, as well as recording the ground reaction forces. From the recorded marker data, participants' joint motion was calculated through the inverse kinematics using the Human Body Model (HBM) (van den Bogert 2013). Nine participants (Table 1) whose

data is in high quality (less marker missing) were selected from the whole experimental dataset. For the controller identification, ten seconds of perturbed walking data was selected for each participant at each walking speed.

Table 1 - Information about the selected nine participants. There are four females and five males. They are all young adults with the average age of 24. There are two male participants with over-weighted BMI and one male participant in Obesity. All other participants are in normal weight category.

Id	Gender	Age (year)	Height (m)	Mass (kg)	Original Id
1	Female	29	1.72	64.5 ± 0.8	7
2	Female	32	1.62	54 ± 2	3
3	Female	21	1.70	58 ± 2	13
4	Female	28	1.69	56.2 ± 0.6	16
1	Male	20	1.57	74.9 ± 0.9	8
2	Male	20	1.69	67 ± 2	9
3	Male	23	1.73	71.2 ± 0.9	5
4	Male	26	1.77	86.8 ± 0.6	6
5	Male	19	1.77	92 ± 0.2	10

2.2. Human Body Model

The human body model used in the identification is a two dimensional seven-link gait model (Ackermann 2010, Geyer 2010), as shown in Figure 1. It contains an upper body and two legs. Each leg consists of a thigh, a shank, and a foot. The whole upper body was modeled as a single segment. The model has 9 degree of freedoms and 6 controllable joints that driven by torques. In the identification, this model was scaled for each participant based on his/her weight and segment lengths (Winter 2009). The effect of random speed perturbation is modeled inside the contact model between the gait model and the ground. Check the supplementary material S1, for detail information of this human body model.

2.3. Locomotion Controller

The locomotion controller used in this paper has the similar control architecture of M2V2 robot (Pratt 2012) which consisted with two components: the stance leg control and the

swing leg control (Figure 2). Open loop torques were used to control the motion of stance leg. A feedback control system was used to control the motion of swing leg, except that the ankle joint was still controlled by open loop torque. The focus of this paper is to identify control parameters inside the swing leg feedback control loop. Joints controlled by the open-loop torque have the potential to generate any motion, which eventually followed experimental data in the identification. The closed-loop swing leg control system includes four items: a foot placement controller, a swing path generator, an inverse kinematics component, and a local tracking controller.

Figure 1 - Structure of the locomotion control system for the step strategy identification. The stance leg and the ankle joint in swing leg are controlled by open loop torques. The hip and knee joints of swing leg are controlled by the state feedback control loop. The purpose of open-loop torque control is just to let these controlled joints following the experimental data. The focus of this paper is to identify control parameters inside the swing leg control loop.

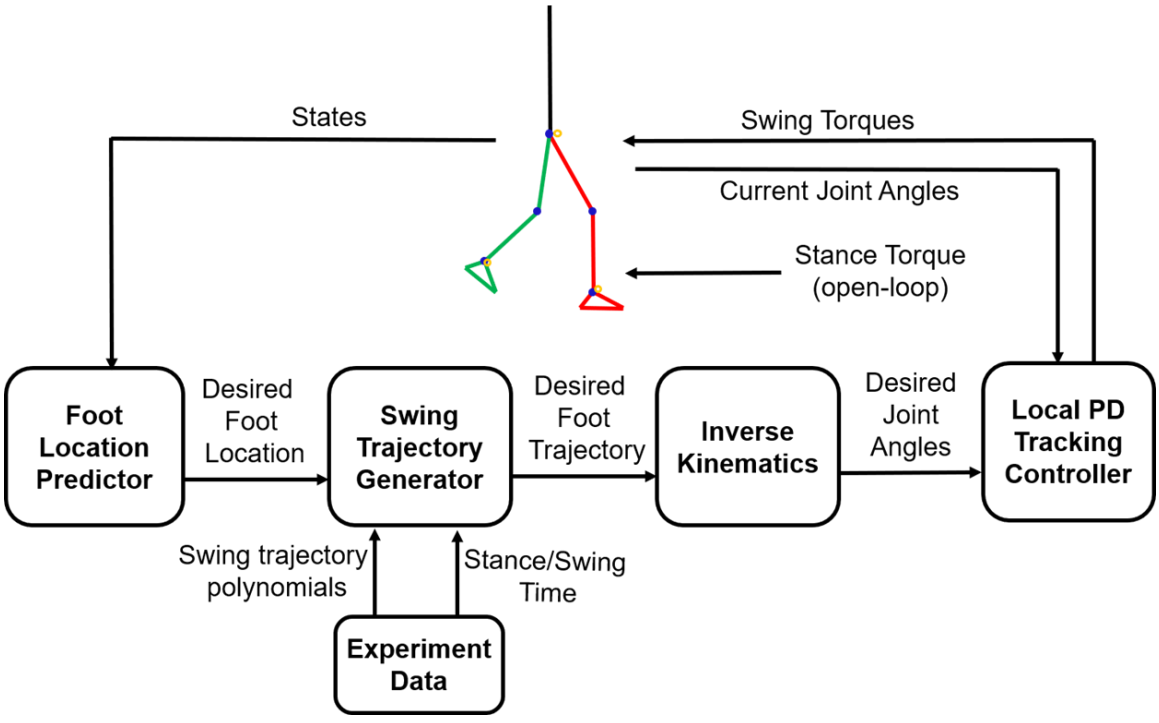

2.3.1. Foot Placement Controller

The function of foot placement controller is to estimate a proper foot placement for the swing leg. We used the same feedback control structure as in the capture theory. The basic foot placement estimation in capture theory is in the form of Equation (2) (Koolen 2012). Standing foot location is the zero reference for other moving parts.

$$\begin{aligned} r_{ic} &= \frac{r}{z_0} + \frac{\dot{r}}{\omega_0 z_0} \\ r_{ic}(\Delta t) &= z_0 \cdot r_{ic}(0) \cdot e^{\omega_0 \cdot \Delta t} \end{aligned} \tag{2}$$

where, r_{ic} is the instantaneous capture point based on the state feedback; r is the CoM position that projected to the ground; z_0 represents the height of CoM in the LIP model; $\dot{r}$ is the horizontal velocity of CoM position; $\omega_0 = \sqrt{g/z_0}$ is the reciprocal of time constant of the LIP model; g represents the gravity; $r_{ic}(\Delta t)$ is the capture point at the coming Δt time point; $r_{ic}(0)$ is the current instantaneous capture point.

In the identification, the same feedback structure was used, but feedback gains were identified from experimental data. The identified foot placement controller is showing in Equation (3) and we used pelvis position and velocity as the feedback signal, instead of the CoM, since they are close. Standing foot location is the zero reference for other moving parts too.

$$\begin{aligned} x_{ifp} &= P_1 \cdot \frac{x_p}{L_{leg}} + P_2 \cdot \frac{\dot{x}_p}{\omega_0 \cdot L_{leg}} \\ x_{fp}(\Delta t) &= L_{leg} \cdot x_{ifp}(0) \cdot e^{\omega_0 \cdot \Delta t} \end{aligned} \tag{3}$$

where, x_{ifp} is the instantaneous desired foot placement based on the pelvis position and velocity feedback; x_p is the relative pelvis position that projected on the ground in sagittal plane; L_{leg} represents the leg length; $\dot{x}_p$ is the horizontal velocity of pelvis; P_1 and P_2 are

the two gains applied on the two feedback signals, which needs identified; $\omega_0 = \sqrt{g/L_{leg}}$ is the reciprocal of the time constant of the human dynamic model; g represents the gravity; $x_{fp}(\Delta t)$ is the desired foot placement at the coming Δt time point; $x_{ifp}(0)$ is the current instantaneous desired foot placement.

2.3.2. Swing Path Generator

The swing path generator calculates the swing trajectory of the swing ankle joint. It is a function of the starting swing position, desired foot placement, and total swing time. Considering that the overall shape of the swing paths is consistent, the normalized polynomial function was used to describe it. The swing path function also decomposed into x and y directions to make each of the function simpler than describing together. Both x and y direction polynomial functions have the same format as showing in Equation (4).

$$f(P_{sta}, P_{des}, T, t) = \sum_{n=1}^{N} A_n * (P_{des} - P_{sta}) \cdot \left(\frac{t}{T}\right)^n \quad (4)$$

where, P_{sta} is the swing foot location at the starting swing time; P_{des} is the estimated foot placement at the ending swing time; T is the total swing time; t is the current swing time; N is the total order of the polynomial function; A_n is the coefficient of the n^{th} order polynomial term.

Coefficients A_n of the polynomial function were optimized over 500 experimental swing paths for each participant at one walking speed. See the supplementary material S2, for detail information of the polynomial coefficients optimization.

2.3.3. Inverse Kinematics

The inverse kinematics module resolves the joint angles of the swing leg to match with the swing foot position at each time frame. Based on the geometry of the leg, the kinematic

function between swing leg joint angles and ankle joint position can be described in Equation (5).

$$\begin{aligned} P_x &= l_{thigh} \cdot sin(\theta_h) + l_{shank} \cdot sin(\theta_h + \theta_k) \\ P_y &= l_{thigh} \cdot cos(\theta_h) + l_{shank} \cdot cos(\theta_h + \theta_k) \end{aligned} \quad (5)$$

where, P_x is the ankle joint position of swing leg in x direction; P_y is the ankle joint position of swing leg in y direction; l_{thigh} is the length of thigh; l_{shank} is the length of shank; θ_h is the hip joint angle; θ_k is the knee joint angle.

2.3.4. Local Tracking Controller

The local tracking controller controls the hip and knee joints to track the calculated joint angles from the inverse kinematics module. Proportional-derivative (PD) control format was used to track the joint motions, shown in Equation (6). The PD control parameters are also optimized in the identification process.

$$\begin{aligned} \tau_h &= Kp_h \cdot \left(\theta_h^{ref} - \theta_h\right) + Kd_h \cdot \left(\dot{\theta}_h^{ref} - \dot{\theta}_h\right) \\ \tau_k &= Kp_k \cdot \left(\theta_k^{ref} - \theta_k\right) + Kd_k \cdot \left(\dot{\theta}_k^{ref} - \dot{\theta}_k\right) \end{aligned} \quad (6)$$

where, τ_h and τ_k are the hip and knee joint torques calculated from local tracking controllers; Kp_h and Kd_h are the proportional and derivative feedback control gains for hip joint; Kp_k and Kd_k are the proportional and derivative feedback control gains for knee joint; θ_h^{ref} and $\dot{\theta}_h^{ref}$ are the reference joint angle and angular velocity of hip joint which are from the inverse kinematics component; θ_h and $\dot{\theta}_h$ are the feedback joint angle and angular velocity of hip joint; θ_k^{ref} and $\dot{\theta}_k^{ref}$ are the reference joint angle and angular velocity of knee joint which are from the inverse kinematics component; θ_k and $\dot{\theta}_k$ are the feedback joint angle and angular velocity of knee joint.

2.4. Indirect Identification Approach

The indirect identification approach finds the desired control parameters by forcing the closed-loop simulation model generating the similar perturbation responses as testing participants'. This can be considered as optimization problem, in which the control parameters are optimized to minimize the difference between the output of simulation model and the experimental data. In this step controller identification, the minimizing parameters are joint trajectories, instead of the foot placements directly. The definition of the human walking step controller identification in the optimization format is shown in Equation (1).

$$\begin{aligned}
&\text{Optimize state trajectories: } x(t) \text{ and control parameters: } P \\
&\text{Minimize the objective function: } F = \int_0^T \|\theta_m(t) - \theta(t)\|^2 dt \\
&\text{Subject to: human system dynamics: } f(x(t), \dot{x}(t), P, v_{belt}) = 0 \\
&\qquad\qquad \text{bounds on state: } x_{low} < x(t) < x_{upp} \\
&\qquad\qquad \text{bounds on control parameters: } P_{low} < P < P_{upp}
\end{aligned} \tag{1}$$

where, $f(x(t), \dot{x}(t), P, v_{belt}) = 0$ represents the dynamic equation of the closed-loop human locomotion system which consisted with the gait model and state feedback locomotion controller; $x(t)$is the plant model state which included joint motions q and joint velocities $\dot{q}$; $\theta(t)$represents the leg joints' motion of the gait model, including hip, knee, and ankle; $P = [P_1, P_2, Kp_h, Kd_h, Kp_k, Kd_k, \tau_{open}]$ represents the control parameters inside the locomotion controller; Open-loop joint torques τ_{open} are also included in control parameters; T is the time length of the identified experimental data; v_{belt} is the velocity of the belt speed including random perturbations in the walking experiment; x_{low} an x_{upp} are

the lower and upper bounds of the human system states; P_{low} and P_{upp} are the lower and upper bounds of the control parameters.

This optimization problem was solved with direct collocation method (Hargraves 1987) and gradient based optimizer Ipopt (Wachter 2006). Detail information of solving the optimization can be found in the supplementary material S3.

The local optimum of this optimization was largely eliminated by selecting the best result from ten optimizations in one identification problem. In this paper, an identification problem was defined as one step controller identification problem on one experiment trial (one walking speed) of a participant. In total, there are 27 identification problems (9 participants, 3 speed trials for each participant). Ten optimizations with random initial guesses were ran for one identification problem. The best identified step controller who can control the plant model generating the closest joint trajectories with experimental data were selected as the best step controller for this identification problem. Overall, 270 optimizations were conducted in this study. They took about 500 computing hours in an Intel i5-8300H CPU.

3. RESULTS

This study identified the step control gains from perturbed walking data. Twenty-five out of twenty-seven identification problems were identified successfully. Table 2 shows the coefficients of determination (R^2) between the identified joint trajectories and the experimental data for all twenty-seven trials. Each number shows the highest R^2 among ten optimizations in one identification problem. Two 'N/A' values in the table indicate unsuccessful identifications, in which no solution was found from optimizations. Except these two, all other identification problems have very high R^2 values, which indicates that

the nonlinear gait model was able to reproduce participants' responses with the identified step controllers. One comparison (participant M5 at 1.2m/s walking speed) of the joint motion between identified result and experimental data is shown in Figure 2. With the high R^2, the joint motion generated by the identified step controller is almost identical to the participant's responses under the same belt speed perturbation. Specifically, almost every large and small variations among gait cycles was matched, instead of only fitting the average motions.

Table 2 - Coefficient of determination (R^2) between identified trajectories and experiment data. 'M' means male subjects; 'F' means female subjects. 'N/A' means the identification problem was not successful.

Speed	F1	F2	F3	F4	M1	M2	M3	M4	M5
0.8 m/s	0.991	0.988	0.983	0.992	0.990	0.982	0.991	0.973	0.964
1.2 m/s	0.992	0.993	0.989	N/A	0.989	0.977	0.991	0.981	0.983
1.6 m/s	0.988	0.988	N/A	0.986	0.979	0.974	0.989	0.983	0.982

Figure 2 - The identified joint trajectories of male participant 5 at walking speed 1.2m/s. The red solid line is the experimental trajectories, and the blue dash line is the identified trajectories.

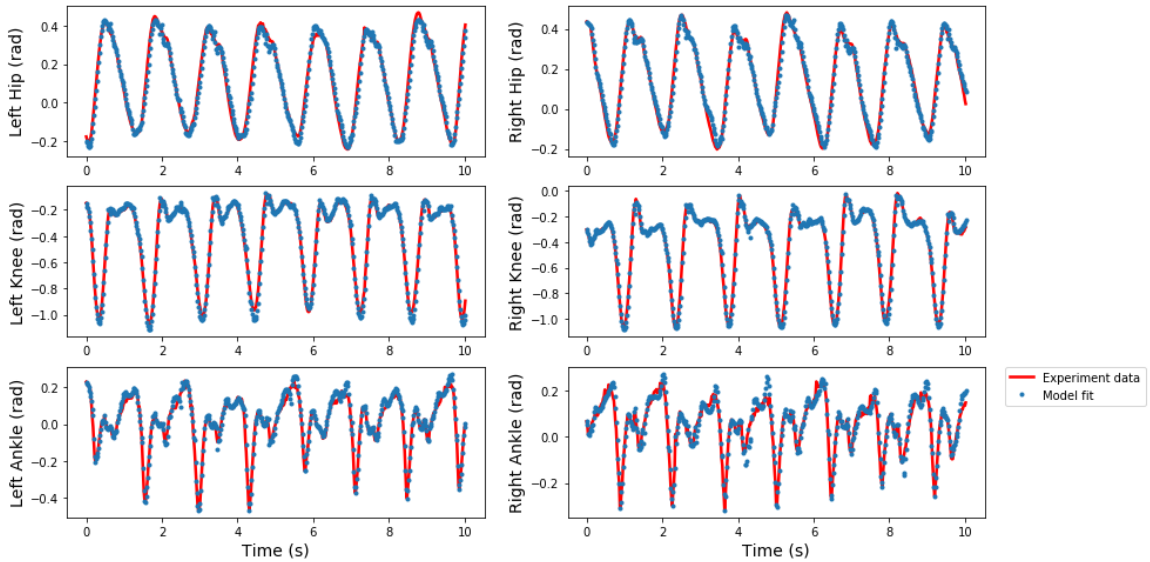

Identified step control gains of nine participants at three walking speeds are shown in Figure 3. There are two gains in the step strategy as motioned in the section 2.4: position gain and velocity gain. These two gains are dimensionless which were normalized by the subjects' leg length L_{leg} and gravity g. In general, the identified gains are close to what the capture theory suggested (grey lines). Specifically, identified position gains have an average value of 0.7 and velocity gains have an average value of 0.85. Both position and velocity gains are smaller than one, which indicates that human tends to choose shorter steps. For each participant, the identified gains of three walking speed are connected with dash-line. Even though there are variations among participants, both single participant's result and overall result clearly illustrate that there are change trends of both position and velocity gains change along with walking speed changes. Position gains have a small increase rate with the increasing of walking speed. While, the velocity gains have a large decrease rate with the increasing of walking speed. This suggests that constant gain in the feedback control structure of capture theory cannot explain the foot placement choice of the testing participants. In addition, control gains of male and female participants are plotted with solid triangle and circles, respectively. There is no significant difference between male and female participants.

Figure 3 - The identified step strategy gains in the foot placement controller. The averaged similar best pelvis position and the velocity gains are showing in the subplot left and right, respectively. Female subjects are marked with solid circle and male subjects are marked with solid triangles. Identified gains in one participant are connected by dash lines.

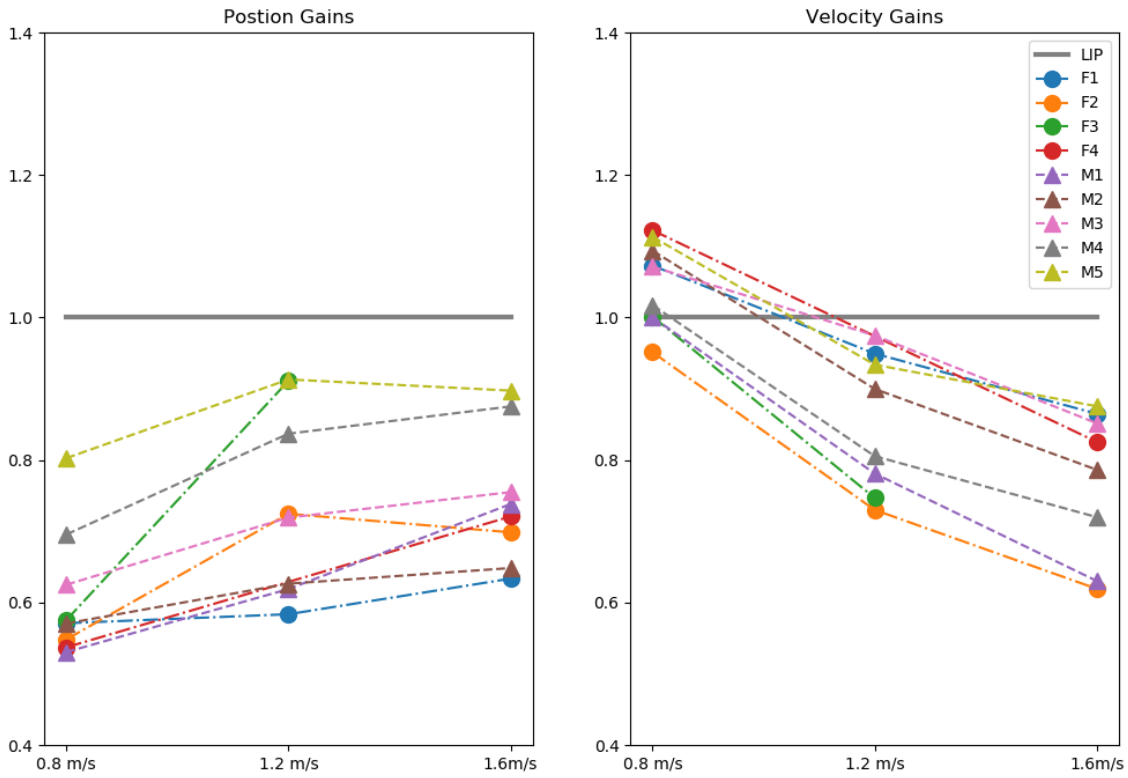

A phase plot of one swing period is showing in Figure 4. Beside the motion of the seven-link gait model, the green dash line is the swing path generated by an identified step controller. The two green dots at the left beginning and the right ending of the green dash line are the starting swing point and the estimated foot placement. The swing path is generated by the normalized polynomial function (mentioned in Section 2.4) based on the above starting and ending dots. This phase plot shows that the swing leg follows the generated swing path very well. More importantly, the desired foot placement calculated by the identified step controller is not a fixed point on the ground but keeps changing based on the participant's motion. For instance, at t = 0.24 second, there is a large change of the desired foot location due to the belt speed perturbation.

Figure 4 - Stick plots of one swing phase. The red leg is the swing leg, and the blue leg is the stance leg. The green dash line is the swing path based on the identified step strategy algorithm. The beginning and ending two green points are the start swing and end swing points.

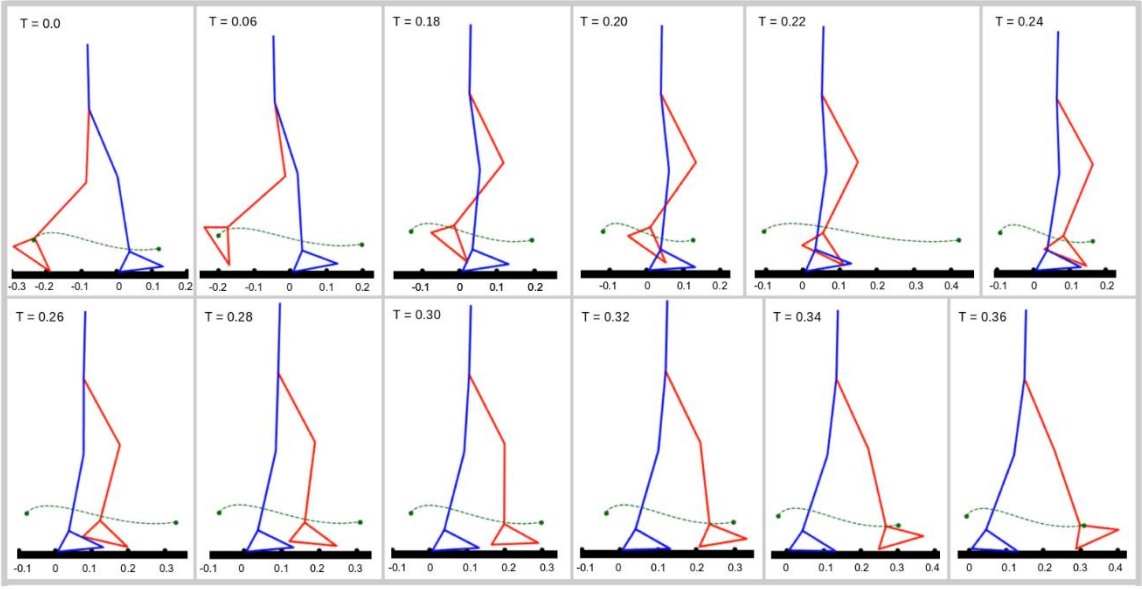

The similarity of ten optimizations and cross-check of the identified step controllers can be found in supplementary material S4 and S5.

4. DISCUSSION

In this study, control gains in the step controller which has the same feedback structure as the capture theory have been identified from the continuously perturbed walking data. In general, both identified position gains and velocity gains are small than "1" which suggests that testing participants chose smaller step lengths than the capture theory suggested. This is consistent with Hof's founding that human step behind the extrapolated center of mass (same as the capture point) (Hof 2008). And this confirmed the conservative of one step capture point, which might be caused by losing forward velocity (captured) and lack of impact model (heel strike). Furthermore, the identified step control gains vary based on the walking speed, which does not match with the constant gains in the capture theory. This

reveals that test participants are using nonlinear feedback functions to estimate the foot placement, instead of the linear function suggested by the capture theory, if considering one step controller for all walking speeds. This difference may come from the simplification of the LIMP that the capture theory used. Even though, we are not able to locate the detail of reasons, this identification results can be reference to help develop more accurate models in foot placement estimation.

However, the findings of the current study do not support one pervious study in human step strategy extraction (Wang 2014). The biggest difference is that they got phase dependency step strategy control gains, while our results show that one constant set of step strategy control gains can already explain the step length changes in the perturbed walking data. One possible reason is that they studied the relationship between the walking status of a specific phase and the foot landing position, which ignored the changes that happened after the studied phase.

The indirect identification approach guaranteed that the identified step controllers are valid in controlling humanoid robots. This is because the nonlinear gait model (represent the human body dynamics) was included in the identification work. In the identification, the gait model served as constraints which forced the identified step strategies having the capability to control the gait model achieving stable and desire motion. This is equivalent to the forward simulation test on a human dynamic model. This is an important reason why we chose the indirect identification approach instead of the direct identification approach.

Reproducing the joint motion is better than just studying the foot placement. Foot placement only happens once in one gait cycle which is accumulated results of all the previous changes or perturbation in the swing. It is impossible to decompose the final foot

placement information into multiple individual contributors. In contrast, the joint motion is continuous information which includes all the adjustments of the desired foot location. Analysis in Section 2.4.1 shows that the shape of the swing phase is relative consistent though the step lengths and swing duration lengths are different. Therefore, changes in the desired foot location will directly affect the swing leg joint motion by shorting or starching the swing path. Through kinematic, the swing leg hip and knee joint angles are directly affected by the changes of swing path.

The time length of swing period was not an optimization parameter in the step strategy identification. We predefined the stance and swing periods for each gait cycle based on the experimental data. One reason of doing this is because we want to keep our large scaling identification problem solvable by gradient based optimizer, in which a consistent structure of the Jacobin is needed. In each of the identification problem, around 10000 parameters and constraints were optimized, in which the size of Jacobin is about 10000×10000. Using the sparse structure to more efficiently store the Jacobin matrix is essential for our identification. The Jacobian structure will change if the number of direct collocation nodes for the stance and the swing phase changed. In addition, adding the swing duration time as an optimizing parameter will make the optimization slower and harder to solve. On the other hand, since the goal of the identification is to reproduce the joint motions, fixing the swing period will automatically guarantee that the swing period is the same as experimental data once a solution is found. It didn't not affect the identified results since swing time is not the target of identification.

Pelvis position and velocity are used in this study to represent the CoM position and velocity. One reason is because the pelvis position and velocity are easier to get from the

gait model that we used. In addition, the CoM position is very close to the pelvis while walking. Besides, only the horizontal position and velocity of the CoM are used for feedback and the trunk rotation is small in walking. Therefore, horizontal position and velocity of the CoM are close enough to the pelvis, and it is acceptable to use the pelvis motion to represent the CoM motion.

The gains in local tracking controllers for the hip and knee joints were also optimized in the step strategy identifications. However, the results of them are not the main concerns in this study. In practice, these local tracking gains are designed based on the body dynamics. In humanoid robots, local tracking controller is usually designed based on the specific structure of the robot hardware and our identified gains cannot provide a good reference. In addition, PD control structure is not the only structure that can achieve the local joint tracking. However, it is better to optimize these gains in our identification work other than pre-select the values, since manually setting the local tracking gains will limit the tracking ability and may affect the identified step strategy controllers.

This study isn't perfect duo to several simplifications. First of all, the estimated foot placement from the identified step controller was the ankle joint position, which does not count the center of pressure (CoP) changes in the feedback control. However, the CoP changes in the closed-loop gait system itself was considered from the motion of ankle joint, which followed the experimental data. The step controller identification which considering CoP changes is possible, since the nonlinear gait model we used has the potential of calculating the CoP. This will be included in our future study. In addition, the identified step controllers in this study were only about the step length, since a two-dimensional gait model was used here. This 2d gait model is relatively computing friendly comparing to

three-dimensional nonlinear gait models. We insisted to use highly nonlinear gait models because they allow us to study joint motions instead of the foot placement only. The advantage of study joint motion comparing to foot placement is mentioned before. With the identification frame work used in this study, it is not hard to identify three-dimensional step controllers also buy using three -dimensional gait model.

5. CONCLUSION

In this study, step controllers that have the same feedback structure as the capture theory were successfully identified from walking experiment data. Identification results suggested that the capture point is not a bad estimation but a little bit conservative in explaining humans' step choice. In addition, human choosing their foot placement does not based on a linear function of the feedback signals, but rather a nonlinear function.

CONFLICT OF INTEREST

The authors of this paper have no financial or personal relationships with other people or organizations that could inappropriately influence (bias) our work.

ACKNOLEDGEMENT

This work was supported by the National Science Foundation under Grant No. 1344954. (Is this number correct?)

REFERENCE

Townsend, M.A., 1985. Biped gait stabilization via foot placement. *Journal of biomechanics, 18*(1), pp.21-38.

Kuffner, J.J., Kagami, S., Nishiwaki, K., Inaba, M. and Inoue, H., 2002. Dynamically-stable motion planning for humanoid robots. *Autonomous Robots*, *12*(1), pp.105-118.

Sugihara, T. and Nakamura, Y., 2002. Whole-body cooperative balancing of humanoid robot using cog jacobian. In *IEEE/RSJ international conference on intelligent robots and systems* (Vol. 3, pp. 2575-2580). IEEE.

Stephens, B., 2007, November. Humanoid push recovery. In *2007 7th IEEE-RAS International Conference on Humanoid Robots* (pp. 589-595). IEEE.

Pratt, J., Carff, J., Drakunov, S. and Goswami, A., 2006, December. Capture point: A step toward humanoid push recovery. In *2006 6th IEEE-RAS international conference on humanoid robots* (pp. 200-207). IEEE.

Kajita, S., Kanehiro, F., Kaneko, K., Yokoi, K. and Hirukawa, H., 2001. The 3D Linear Inverted Pendulum Mode: A simple modeling for a biped walking pattern generation. In *Proceedings 2001 IEEE/RSJ International Conference on Intelligent Robots and Systems. Expanding the Societal Role of Robotics in the Next Millennium (Cat. No. 01CH37180)* (Vol. 1, pp. 239-246). IEEE.

Pratt, J., Koolen, T., De Boer, T., Rebula, J., Cotton, S., Carff, J., Johnson, M. and Neuhaus, P., 2012. Capturability-based analysis and control of legged locomotion, Part 2: Application to M2V2, a lower-body humanoid. *The International Journal of Robotics Research*, *31*(10), pp.1117-1133.

Koolen, T., De Boer, T., Rebula, J., Goswami, A. and Pratt, J., 2012. Capturability-based analysis and control of legged locomotion, Part 1: Theory and application to three simple gait models. *The International Journal of Robotics Research*, *31*(9), pp.1094-1113.

Zhang, L. and Fu, C., 2018. Predicting foot placement for balance through a simple model with swing leg dynamics. *Journal of biomechanics*, *77*, pp.155-162.

Kuo, A.D., Donelan, J.M. and Ruina, A., 2005. Energetic consequences of walking like an inverted pendulum: step-to-step transitions. *Exercise and sport sciences reviews*, *33*(2), pp.88-97.

Hof, A.L., Gazendam, M.G.J. and Sinke, W.E., 2005. The condition for dynamic stability. *Journal of biomechanics*, *38*(1), pp.1-8.

Hof, A.L., 2008. The ‘extrapolated center of mass’ concept suggests a simple control of balance in walking. *Human movement science*, *27*(1), pp.112-125.

Geyer, H. and Herr, H., 2010. A muscle-reflex model that encodes principles of legged mechanics produces human walking dynamics and muscle activities. *IEEE Transactions on neural systems and rehabilitation engineering*, *18*(3), pp.263-273.

Song, S. and Geyer, H., 2013, July. Generalization of a muscle-reflex control model to 3d walking. In *2013 35th Annual International Conference of the IEEE Engineering in Medicine and Biology Society (EMBC)* (pp. 7463-7466). IEEE.

Song, S. and Geyer, H., 2015. A neural circuitry that emphasizes spinal feedback generates diverse behaviours of human locomotion. *The Journal of physiology*, *593*(16), pp.3493-3511.

Wang, Y. and Srinivasan, M., 2014. Stepping in the direction of the fall: the next foot placement can be predicted from current upper body state in steady-state walking. *Biology letters*, *10*(9), p.20140405.

Seethapathi, N. and Srinivasan, M., 2019. Step-to-step variations in human running reveal how humans run without falling. *eLife*, *8*, p.e38371.

van der Kooij, H., van Asseldonk, E. and van der Helm, F.C., 2005. Comparison of different methods to identify and quantify balance control. *Journal of neuroscience methods*, *145*(1-2), pp.175-203.

Moore, J.K., Hnat, S.K. and van den Bogert, A.J., 2015. An elaborate data set on human gait and the effect of mechanical perturbations. *PeerJ*, *3*, p.e918.

Van den Bogert, A.J., Geijtenbeek, T., Even-Zohar, O., Steenbrink, F. and Hardin, E.C., 2013. A real-time system for biomechanical analysis of human movement and muscle function. *Medical & biological engineering & computing*, *51*(10), pp.1069-1077.

Ackermann, M. and Van den Bogert, A.J., 2010. Optimality principles for model-based prediction of human gait. *Journal of biomechanics*, *43*(6), pp.1055-1060.

Cheng, K.B., Huang, Y.C. and Kuo, S.Y., 2014. Effect of arm swing on single-step balance recovery. *Human movement science*, *38*, pp.173-184.

Winter, D.A., 2009. *Biomechanics and motor control of human movement*. John Wiley & Sons.

TABLES and FIGURES

Supplemental Material

Supplementary Information Appendix for: Identification of the Phase Independent Anterior-posterior Step Strategy in Human Walking

Huawei Wang and Antonie J. van den Bogert

Mechanical Engineering, Washkewicz College of Engineering Cleveland State University, U.S.

The appendix contains the following sections:

- Section S1 lists the dynamic equations of the nonlinear gait model described in Figure 1 of the main manuscript.
- Section S2 provides the information about the normalized polynomial function for the swing phase generator
- Section S3 provides the trajectory optimization problem in the direct collocation format
- Section S4 gives information of the similarity of the identified step control gains among ten optimizations.
- Section S5 provides information of the cross-check.

S1 Dynamic equation of the nonlinear gait model

Gait Model Dynamics. The gait model used in this study is a two dimensional seven-link dynamics model (Figure 1), which has been used in many gait studies [1-2]. The dynamic equation of this seven-link gait model was generated using Kane's method through AUTOLEV [3]. The dynamic equation is in the format of general robotics: $M(q)\ddot{q} + C(q,\dot{q})\dot{q} + G(q) = T_{joint} + T_{grf}$, where $q = \left[x, y, \theta_{trunk}, \theta_{Lhip}, \theta_{Lknee}, \theta_{Lankle}, \theta_{Rhip}, \theta_{Rknee}, \theta_{Rankle}\right]^T$ represents motion variables of the gait model, including pelvis motion and joint angles; M represents the mass matrix of the gait model and is a function of motion variables q; C represents the Coriolis matrix and is a function of motion variables q and velocity variables v; G represents the gravity matrix and is a function of motion variables q; T_{joint} represents the external joint torques and T_{grf} represents the effect of ground reaction force applied on the gait model.

Contact Model. The contact model between the gait model and ground is modeled as a nonlinear spring-damper system in the vertical direction [2]. In the horizontal direction, a coulomb friction model that smoothed by a logistic function was included. The effect of speed perturbation in this gait model is modeled as relative speed changes in the contact model. In each foot, there are two contact points (heel and toe). The vertical and horizontal contact forces are calculated from the following equations.

$$F_y = K_p \cdot d \cdot \left(1 - K_d \cdot \dot{d}\right)$$

$$F_x = - C_{friction} \cdot F_y \cdot \left(\frac{2}{1 + e^{\frac{-(v_x - v_{ground})}{v_0}}} - 1 \right)$$

where, F_y is the vertical contact force; F_x is the horizontal contact force; K_p is the stiffness of the ground; $d = \frac{\sqrt{y^2+\sigma^2} - y}{2}$ is the constraint vertical position of contact point, which limited that valuable vertical ground reaction force only exist when contact point interact with ground; K_d is the damping property of the ground; $\dot{d}$ is the constraint vertical velocity of the contact point; $C_{friction}$ is the horizontal friction coefficient of the ground; v_x is the horizontal velocity of the contact point; v_{ground} is the horizontal velocity of the ground; v_0 is the parameter which determines how large the difference between contact point velocity and ground velocity when friction force appears.

The contact model was modeled with continuous functions in which gradients are always exist. This guaranteed that the plant model in loop optimization can be solved by gradient based method. Considering that ground contact forces are functions of the position and velocity of contact point which are functions of the gait model state, the dynamic equation of the gait model with ground contact can be written in the format of $M(q)\ddot{q} + C(q,\dot{q})\dot{q} + G(q) - E\left(q,\dot{q},v_{ground}\right) = T_{joint}$. In which the contact model is included in the $E\left(q,\dot{q},v_{ground}\right)$ component.

Closed-loop Model. The step controller identified in this study is a state feedback controller which has the format of $T_{joint} = f(P,q,\dot{q})$, in which P represents control parameters. Combine this state feedback controller with gait model and contact model, the dynamic equation of the closed-loop system can be written as $M(q)\ddot{q} + C(q,\dot{q})\dot{q} + G(q) - E\left(q,\dot{q},v_{ground}\right) - f(P,q,\dot{q}) = 0$. In simplification, it can be written in the format of: $F\left(q,\dot{q},\ddot{q},P,v_{ground}\right) = 0$.

S2 Normalized polynomial function for the swing foot

The swing foot trajectory is described as normalized polynomial functions in both vertical and horizontal directions. Coefficients of the polynomial function were optimized to fit with the swing paths in experimental data. For each participant at one walking speed, swing paths from over 500 gait cycles were used to optimize the coefficients. An example of the swing paths from one participant at one walking speed are showing in Figure 1. The swing path is relative motion which is relative to the pelvis point

Figure 1 - Swing trajectories from the experimental data. Subplot 1) shows the swing trajectory in the swing phase. It starts at the swing starting position and finishing at the touch down point. Subplot 2) shows the swing trajectory shape in the x and y directions over 500 gait cycles. The swing path of the ankle joint is relative to the pelvis position.

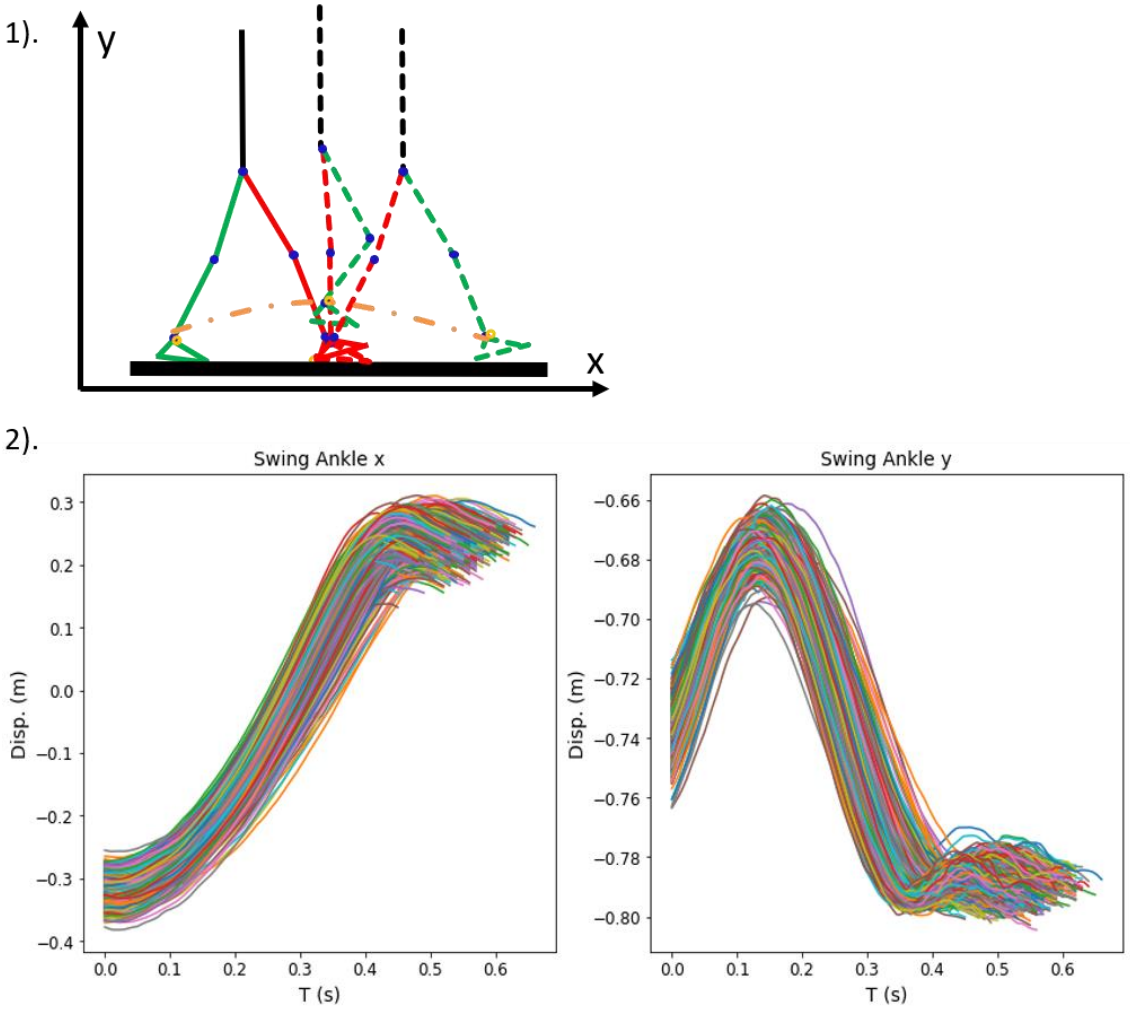

The optimization problem of the polynomial coefficients is regular optimization problem which is defined in follow:

Optimize coefficients A_n

Minimizing the objective function:

$$obj = \sum_{i=1}^{M} \int_{t=0}^{T_i} (f_{path}^{i}(t) - f_{polynomial}^{i}(A_n, t))^2 \cdot dt$$

Subject to: $f_{polynomial}^{i}(A_n, 0) = f_{path}^{i}(0), for\ i = 1, 2, \ldots, M$

$$f_{polynomial}^{i}(A_n, T) = f_{path}^{i}(T), for\ i = 1, 2, \ldots, M$$

where, A_n represents coefficients of the polynomial function; M represents the total number of the experimental swing paths; $f_{path}^{i}(t)$ represents the i^{th} experimental swing path; T_i represents the swing time length for the i^{th} experimental swing path; $f_{polynomial}^{i}(A_n, t) = \sum_{n=1}^{N} A_n * \left(f_{path}^{i}(T) - f_{path}^{i}(0)\right) \cdot \left(\frac{t}{T_i}\right)^n$ represents the path generated by the normalized polynomial function for the i^{th} experimental swing path with the coefficients A_n;

Constraints of the optimization guaranteed that the normalized polynomial function starting and ending with the same values as experimental swing paths. The optimization problem is solved by using the *minimize* function in *python scipy.optimize* package [4]. Different orders of the polynomial functions, from first and sixth, were optimized to find the number of orders that holds the best fit. Based on the fitting results, fifth order polynomials are selected for both x and y directions of the swing path. RMS of different orders of the normalized polynomial functions with experimental data and one example of the swing path fit are shown in Figure 7.

Figure 5 - Fits between the optimized polynomial functions and the experimental swing paths. Subplot 1) shows the means and standard deviation of the difference between the polynomial functions and experimental data. Fit get better with the increase of the degree of polynomial functions. Subplot 2) shows one example of the fit for one optimized polynomial function. In which, the best, median, and worst fits in over 500 experimental swing trajectories are shown.

1).

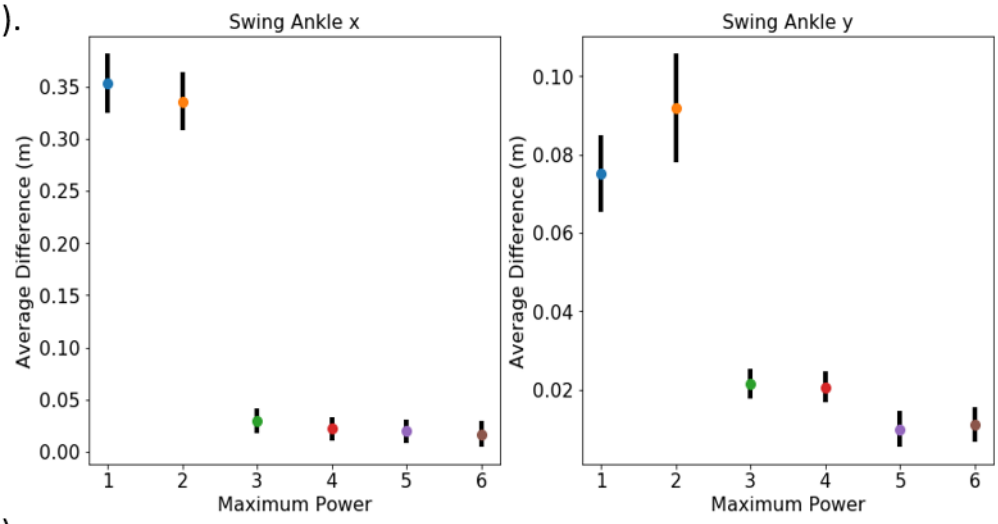

2).

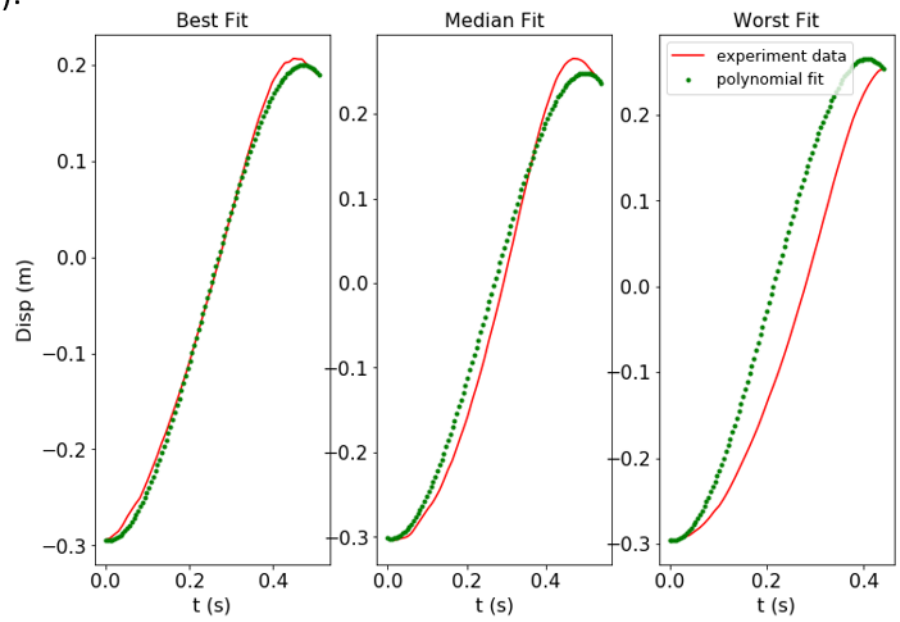

S3 Solving the identifications as nonlinear programing problems

As mentioned in the main manuscript, the identification problem is also a trajectory optimization problem. In order to solve the trajectory optimization, the direct collocation method was used in this paper. It transformed the trajectory optimization problem into a nonlinear program (NLP) with a finite number of unknowns: the state vector x at N

collocation nodes, and the controller parameters P. Backward Euler approximation was used to convert the body dynamics constraint into a series of constraints:

$$\text{Optimize Y} = [x_1,\ x_2,\ \ldots,\ x_N,\ P]$$

$$\text{Minimize } F(Y) = \sum_{i=1}^{N} \|x_i^m - x_i\|^2$$

$$\text{Subject to: h(Y)} = \begin{cases} \begin{bmatrix} F(x_2,\ \dot{x}_1,\ P,\ v_{belt,2}) = 0 \\ \ldots \\ F(x_N,\ \dot{x}_{N-1},\ P,\ v_{belt,N}) = 0 \end{bmatrix} \\ \begin{bmatrix} x_1^{low} \le x_1 \le x_1^{upp} \\ \ldots \\ x_N^{low} \le x_N \le x_N^{upp} \end{bmatrix} \\ P_{low} \le P \le P_{upp} \end{cases}$$

The direct collocation method used in this paper helped avoid forward simulation of the nonlinear gait model by setting up constraints [5]. Forward simulation of this nonlinear gait model could be painful, since fall could be a big issue. In the format of nonlinear programing, many commercial optimizers can be used to solve them efficiently. In the direct collocation, the number of collocation nodes was set as 50 per second, and gradient based interior pointer optimizer IPOPT was used to solve the NLP [6].

S4 Similarity of the identified control gains among ten optimizations

To increase the confidence that the identified step strategies are not a bad local optimum result, how many times the similar best results appeared in each identification problem (ten optimizations) were checked (Table 2). The similar best results were defined within 5% variation when comparing the root-mean-square (RMS) of the difference between the identified trajectories and the experimental data. In most identification problems, the similar best results were found more than once, which suggests that the identified step

controllers are more likely not the bad local solutions. The standard deviation of the control gains in the corresponding best similar results are shown in Table 4 and Table 5. In general, they are less than 5%, which means that the identified step strategies among the similar best fits are similar. This, in another aspect, suggests that the identified step controllers are good results.

Table 3 - The number of similar best results in each identification problem. In most of the identification problems, similar best results were found more than once. Only six out of twenty-seven identification problems found one similar best result. There are two identification problems which were not successful in finding feasible results.

Speed	F1	F2	F3	F4	M1	M2	M3	M4	M5
0.8 m/s	4	2	2	1	7	5	5	1	1
1.2 m/s	4	8	2	0	4	2	3	9	3
1.6 m/s	2	1	0	1	7	2	1	8	2

Table 4 - The standard deviation of the similar best results as a percentage of the averaged position feedback gains. For the identification problems which have no solution, or only one best result, there is no standard deviation and 'N/A' was wrote.

Speed	F1	F2	F3	F4	M1	M2	M3	M4	M5
0.8 m/s	5.34%	4.21%	2.47%	N/A	2.34%	2.44%	3.56%	N/A	N/A
1.2 m/s	3.39%	1.66%	1.58%	N/A	0.69%	0.45%	3.80%	2.56%	1.17%
1.6 m/s	0.43%	N/A	N/A	N/A	1.73%	1.82%	N/A	1.53%	0.16%

Table 5 - The standard deviation of the similar best results as a percentage of the averaged velocity feedback gains. For the identification problems which have no solution, or only one best result, there is no standard deviation and 'N/A' was wrote.

Speed	F1	F2	F3	F4	M1	M2	M3	M4	M5
0.8 m/s	0.14%	0.13%	0.49%	N/A	0.69%	0.71%	0.67%	N/A	N/A
1.2 m/s	0.30%	1.62%	1.81%	N/A	0.45%	0.54%	1.93%	1.97%	1.68%
1.6 m/s	0.65%	N/A	N/A	N/A	0.60%	0.34%	N/A	1.29%	0.30%

S5 Cross check of the identified control gains

To make sure that ten seconds experimental data is sufficient to identify the two feedback gains in the step controllers, cross check of the identified control gains was done. Beside the ten seconds perturbed walking data used in the identification in the main manuscript, we also identified the step strategy on another ten- and twenty-seconds perturbed walking data, which did not show significant differences with the results on the ten seconds data (Figure 8). One-way ANOVA tests showed that there is no significant difference ($P > 0.05$) between the three periods. Tests on the gains of different speeds showed that there is significant difference ($P < 0.05$ for position gain, $P < 0.05$ for velocity gains) between three speeds. Since joint motion is the reproducing target in this research, instead of the foot placement, ten seconds perturbed walking data contains enough information for identifying the two feedback gains.

Figure 8 – Comparison of the identified control gains among three periods of experimental data. In which, period 1 is the 10 seconds experimental data mentioned in the Result section; period 2 is the 20 seconds experimental data which includes the period 1 data; period 3 is another 10 seconds experimental data away from the period 1 and 2. There is no significant difference of the identified control gains among the three data periods. However, there is a significant difference of the identified control gains among the three speeds.

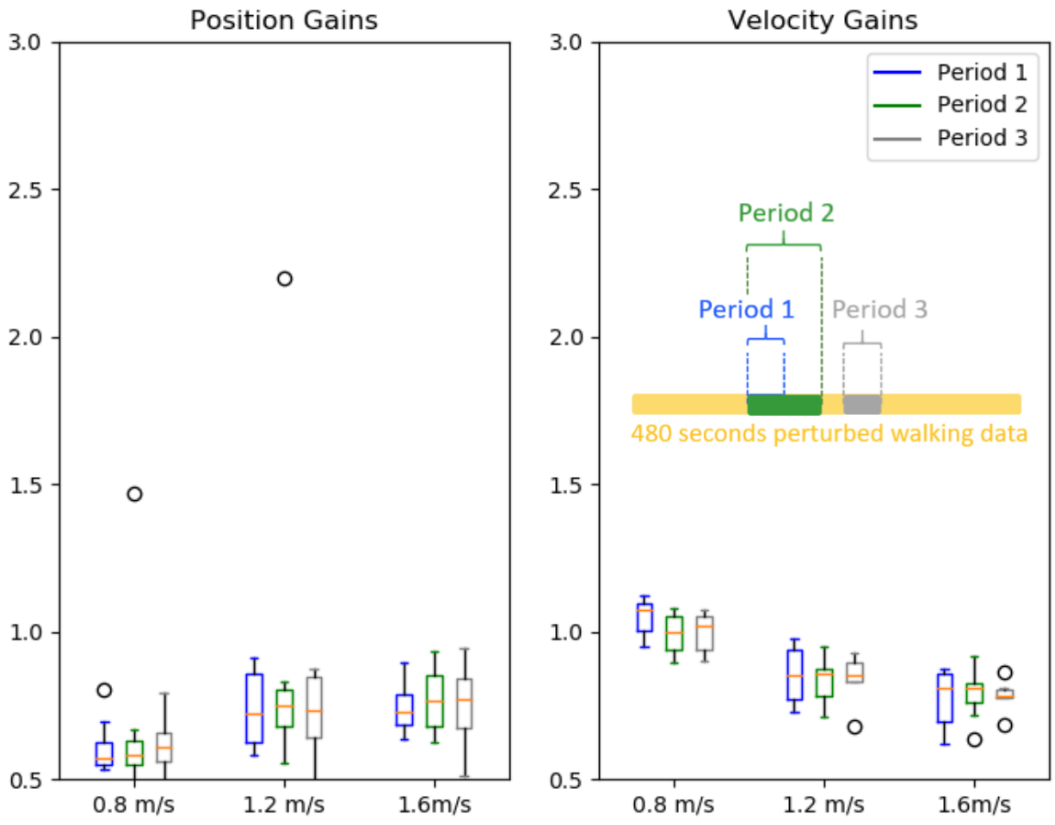

Reference

[1]. Geyer, H. and Herr, H., 2010. A muscle-reflex model that encodes principles of legged mechanics produces human walking dynamics and muscle activities. *IEEE Transactions on neural systems and rehabilitation engineering*, *18*(3), pp.263-273.

[2]. Ackermann, M. and Van den Bogert, A.J., 2010. Optimality principles for model-based prediction of human gait. *Journal of biomechanics*, *43*(6), pp.1055-1060.

[3]. Levinson, David A., and Thomas R. Kane. "AUTOLEV—a new approach to multibody dynamics." *Multibody systems handbook*. Springer, Berlin, Heidelberg, 1990. 81-102.

[4]. Jones E, Oliphant E, Peterson P, et al. SciPy: Open Source Scientific Tools for Python, 2001, http://www.scipy.org/

[5]. Kelly, Matthew. "An introduction to trajectory optimization: How to do your own direct collocation." *SIAM Review* 59.4 (2017): 849-904.

[6] A. Wächter and L. T. Biegler, On the Implementation of a Primal-Dual Interior Point Filter Line Search Algorithm for Large-Scale Nonlinear Programming, *Mathematical Programming* 106(1), pp. 25-57, 2006